Supplementary Information

Simultaneous manipulation of scalable absorbance and electronic bridge for efficient CO_2 photoreduction

*Xin Zhou[a,#], Xin Zhang[a,#], Penghui Ding[b], Kang Zhong[c], Jinman Yang[c], Jianjian Yi[a], Qingsong Hu[a], Ganghua Zhou[a], Xiaozhi Wang[a], Hui Xu[c,] *, Xingwang Zhu[a,]**,

[a] College of Environmental Science and Engineering, College of Mechanical Engineering, Yangzhou University, Yangzhou 225009, P.R China

[b] Department of Science and Technology, Linköping University, Norrköping SE-601 74, Sweden

[c] School of the Environment and Safety Engineering, Institute for Energy Research, Jiangsu University, Zhenjiang 212013, P.R China

*Corresponding author.

E-mail addresses: zxw@yzu.edu.cn (X. Zhu); xh@ujs.edu.cn (H. Xu)

[#]These authors contributed equally.

Characterization of the photocatalysts

X-ray diffraction (XRD, AXS D8 ADVANCE, Bruker) patterns were recorded by using a Philips X'Pert Pro Super diffractometer with Cu Kα radiation (λ = 1.54178 Å). X-ray photoelectron spectroscopy (XPS, ESCALAB 250Xi, Thermo Fisher) measurements were performed on a VGESCALAB MK II X-ray photoelectron spectrometer with an excitation source of Mg Kα (1253.6 eV). The binding energies obtained in the XPS spectral analysis were corrected for specimen charging by referencing C 1s to 284.8 eV. The field emission scanning electron microscopy (SEM) images were performed by using a FEI Sirion-200 SEM. Transmission electron microscopy (TEM) and high-resolution TEM images were obtained by using a JEOL-2010 TEM with an acceleration voltage of 200 kV. UV-vis diffuse reflectance spectroscopy (DRS) was recorded on a Solid 3700 UV/Vis-NIR spectrophotometer (Shimadzu, Japan). Fourier transform infrared (FT-IR) spectra were acquired on a NICOLET FT-IR spectrometer with KBr tablets, scanning from 4000 to 400 cm^{-1} at room temperature (Thermo Fisher Scientific, America). The electron paramagnetic resonance (EPR) was detected on A300-10/12 Bruker EPR spectrometer. The surface properties of the as-synthesized products were examined by measuring the contact angles of water droplet on the corresponding samples with a XG-CAMB2 instrument. Room temperature photoluminescence (PL) and the decay time spectra were recorded on a Hitachi F-7000 fluorescence spectrophotometer (FLS920, Edinburgh Instruments Ltd.)

Computational methods

In this work, density functional theory (DFT) calculations were performed for structural optimization as implemented in the Vienna ab-initio Simulation Package (VASP). The PBE exchange-correlation functional of the generalized gradient approximation (GGA) was used to describe the exchange correlation energy. To achieve the accurate density of the electronic states, the plane wave cutoff energy was 520 eV and the Brillouin zone integration was performed using Monkhorst-Pack grids of 3×3×1 during the iterations. Ionic relaxations were carried out under the conventional energy (1×10^{-5} eV) and force (0.02 eV/Å) convergence criteria. The ground state structures of CO_2*, COOH* and CO* adsorbed on g-C_3N_4 surface were determined by testing all the possible configurations on possible active sites and found the lowest energy one. The free energy for adsorbates and non-adsorbed gas-phase molecules is calculated as:

$$\Delta G = E_{total} - E_{slab} - E_{mol} + \Delta E_{ZPE} - T\Delta S \qquad (S1)$$

where E_{total} is the total energy for the adsorption state, E_{slab} is the energy of pure surface, E_{mol} is the energy of adsorption molecule, ΔE_{ZPE} is the zero-point energy change and ΔS is the entropy change.

Based on Table S3, calculate the ΔE_{ZPE} and $T\Delta S$ of CO_2 reaction paths:

$$CO_2 + * \rightarrow * CO_2 \qquad T\Delta S = -0.42\ eV;\ \Delta ZPE = -0.14\ eV \quad (S2)$$

$$* CO_2 + H^+ + e^- \rightarrow * COOH \qquad T\Delta S = -0.33\ eV;\ \Delta ZPE = 0.22\ eV \quad (S3)$$

$$* COOH + H^+ + e^- \rightarrow * CO + H_2O \qquad T\Delta S = 0.50\ eV;\ \Delta ZPE = 0.22\ eV \quad (S4)$$

$$* CO \rightarrow * CO\uparrow + * \qquad T\Delta S = 0.46\ eV;\ \Delta ZPE = -0.18\ eV \quad (S5)$$

Photoelectrochemical test

An electrochemical workstation (Chenhua Instruments Company, China) was used to perform electrochemical measurements using a three-electrode system. Photocurrent and electrochemical impedance spectroscopy (EIS) measurements of samples were carried out in the three-electrode system. In the three-electrode system, the reference electrode was a silver and silver chloride, and the platinum wire was used as the counter electrode. The working electrode was prepared as follows: 5 mg of photocatalyst powder was dispersed in 1 mL ethanol solution, then 20 μL of the dispersed solution was coated in a 10 × 5 mm indium tin oxide (ITO) glass and dried under 60°C to remove ethanol for 12 hours. The electrolyte solution is 0.2 M Na_2SO_4. The light source is a 300 W Xenon lamp (PLS-FX300HU, Beijing Perfectlight).

Photocatalytic CO_2 reduction measurement

The photocatalytic CO_2 reduction activities of the as-obtained samples were assessed in a liquid-solid reaction system with a 300 mL closed quartz reactor (CEL-SPH2N). Typically, 10 mg of the sample was dispersed in 10 mL acetonitrile (CH_3CN) aqueous solution (V_{CH3CN}: V_{H2O} = 3 : 2), and then, 2 mL of triethanolamine (TEOA) was added as the hole sacrificial regent, followed by degasification to eliminate the air. The temperature was kept at 10°C and the pressure was kept at 75 kPa. Under CO_2 atmosphere, a 300 W Xenon lamp (CEL-HXF300-T3, Beijing China Education Au-light Co., Ltd., China) was used to initiate the photocatalytic CO_2 reaction. A gas chromatograph (GC7920, Ar carrier) equipped with a thermal conductivity detector

(TCD) and hydrogen flame ionized detector (FID) was used to determine the amount of the gas product. The selectivity of CO and CH_4 was calculated by follow equation: selectivity of CO (%) = $[2v(CO)]/[2v(CO) + 8v(CH_4) + 2v(H_2)] \times 100\%$, and selectivity of CH_4 (%) = $[8v(CH_4)]/[2v(CO) + 8v(CH_4) + 2v(H_2)] \times 100\%$, where $v(CO)$, $v(CH_4)$ and $v(H_2)$, represent the yielding rates for CO, CH_4 and H_2, respectively.

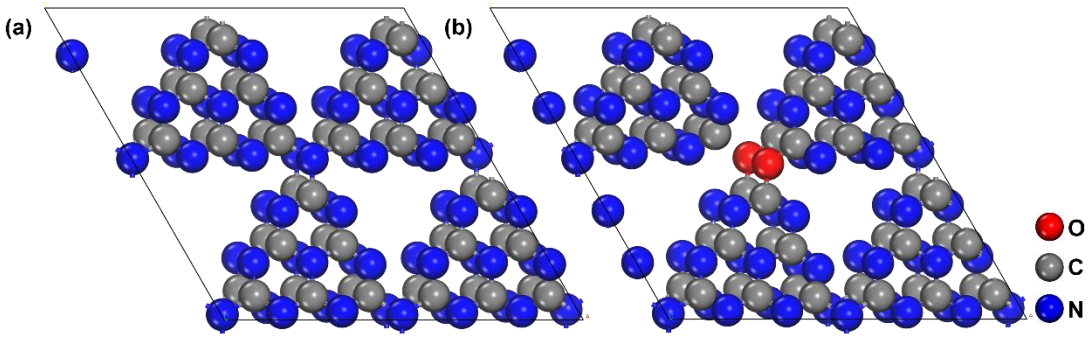

Figure S1. Surface structure of (a) Bulk CN and (b) CSCN.

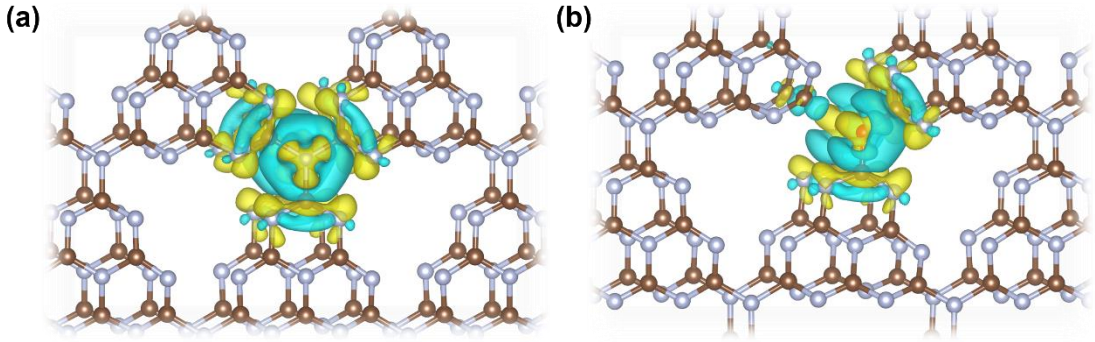

Figure S2. Charge density difference of O and N adsorbed on (a) Bulk CN and (b) CSCN.

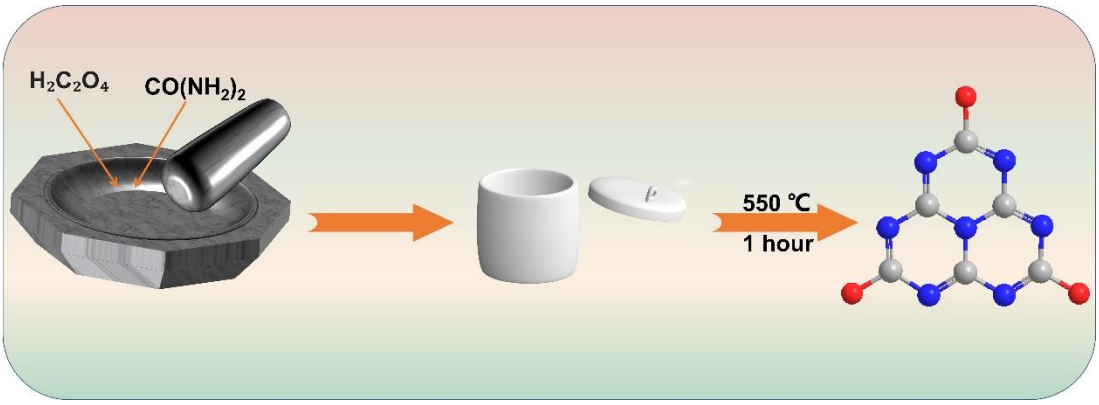

Figure S3. Schematic illustration for preparing CSCN photocatalysts.

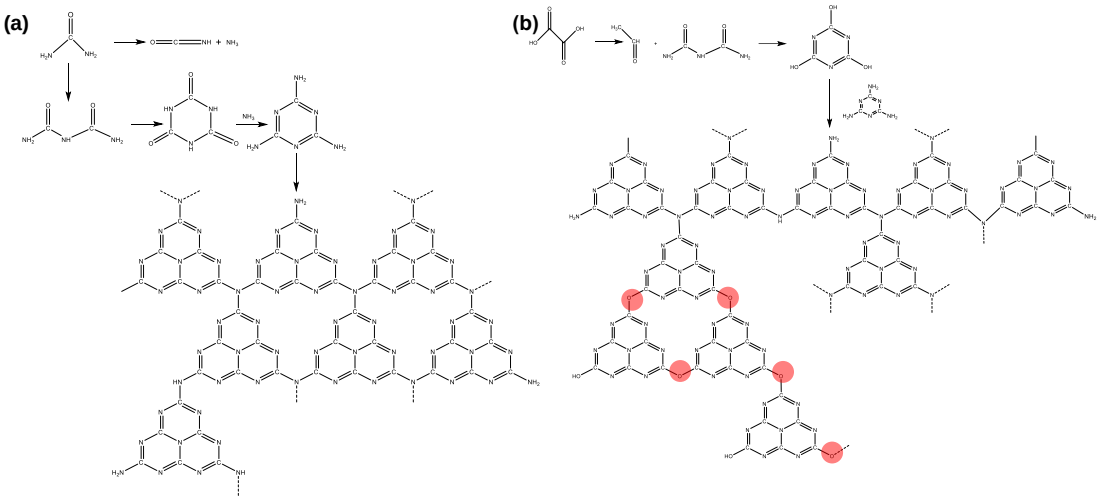

Figure S4. Proposed mechanism of the reaction paths for the formation of polymeric.

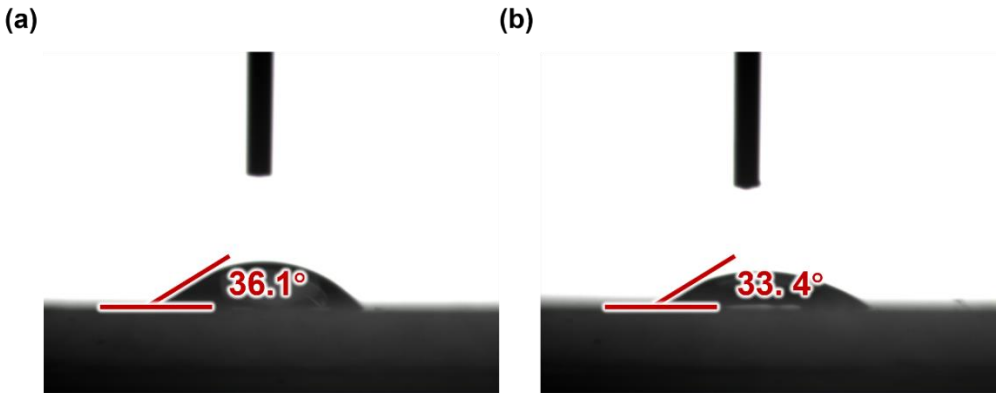

Figure S5. Static water contact angle experiments of (a) Bulk CN and (b) CSCN-2.

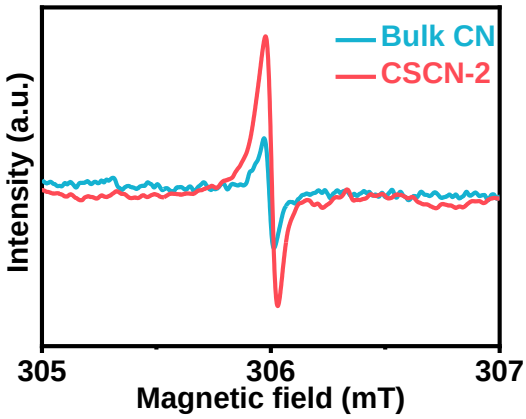

Figure S6. EPR patterns of Bulk CN and CSCN-2 photocatalysts.

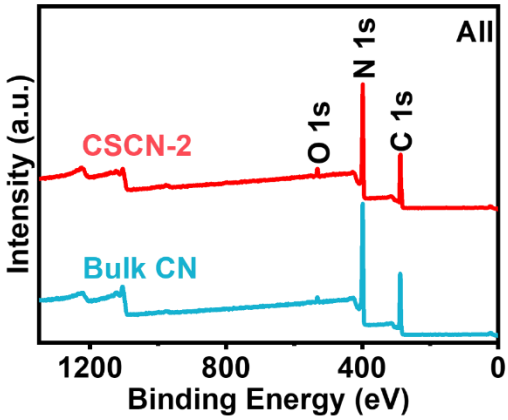

Figure S7. XPS survey spectra of Bulk CN and CSCN-2.

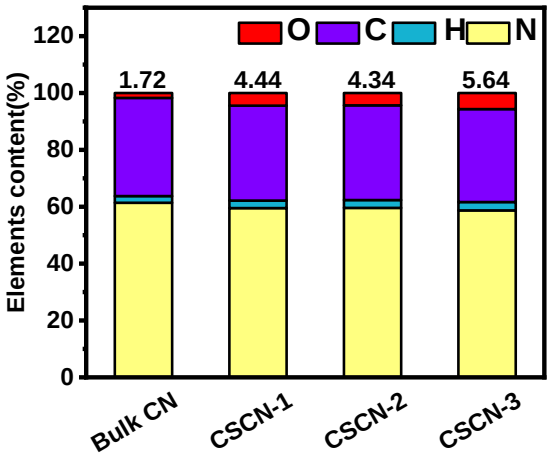

Figure S8. Elemental analysis chart of Bulk CN and CSCN samples.

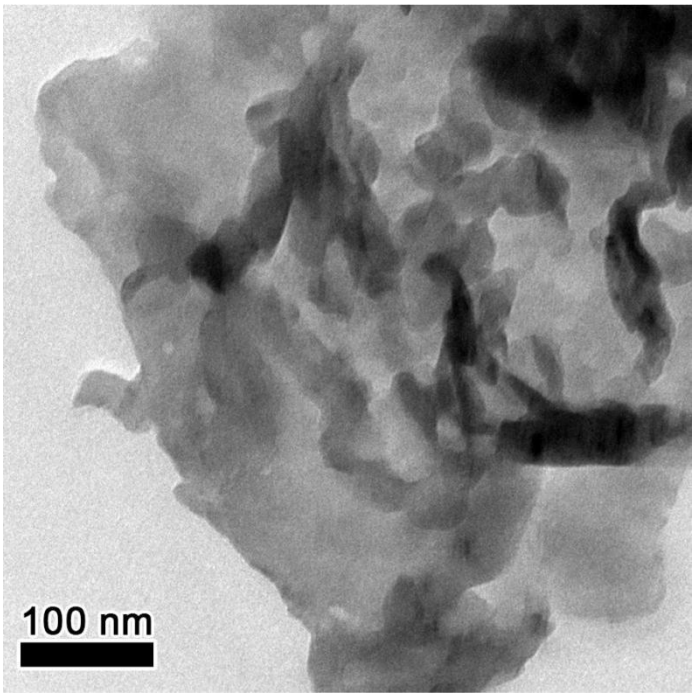

Figure S9. TEM image of Bulk CN.

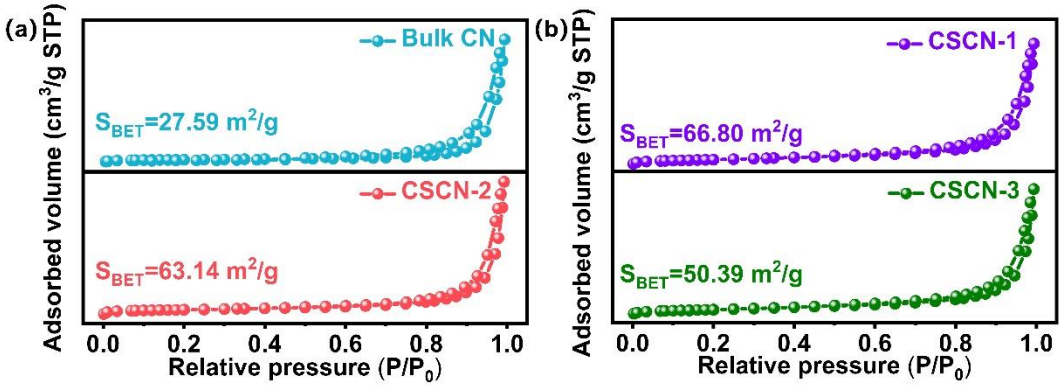

Figure S10. Nitrogen adsorption-desorption isotherms of Bulk CN and CSCN samples.

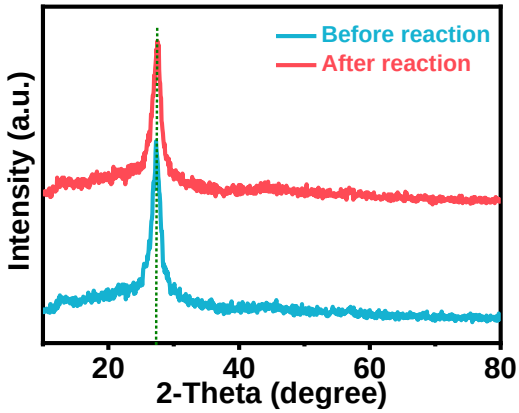

Figure S11. XRD patterns of CSCN-2 before and after the cycling photocatalytic experiment.

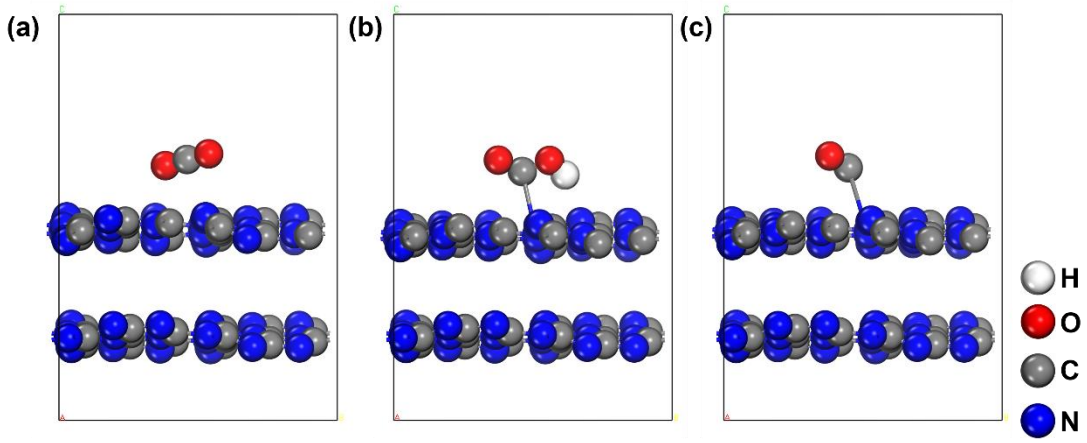

Figure S12. Structural models of Gibbs free energy calculations on Bulk CN surface.

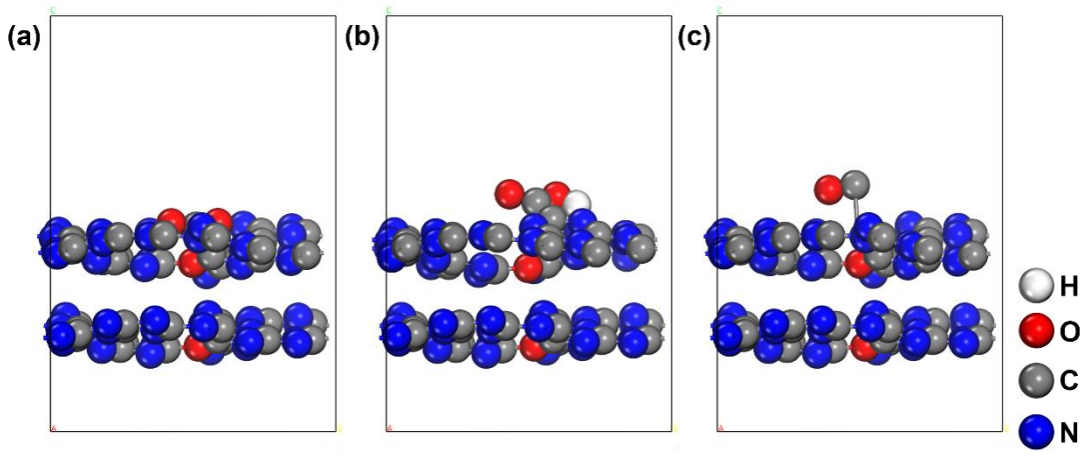

Figure S13. Structural models of Gibbs free energy calculations on CSCN surface.

Table S1. Comparison of photocatalytic CO_2 reduction performances on the state-of-the-art photocatalysts.

Photocatalyst	Reaction medium	Main products ($\mu mol\ h^{-1}\ g^{-1}$)	Ref.
CSCN	300 W Xe-lamp, 2 mL TEOA, 4 mL H_2O, 6 mL acetonitrile, 10 mg catalyst	28.5 (CO)	**This work**
Covalent triazine framework/g-C_3N_4	300 W Xe-lamp, 1 mL $Co(bpy)_3Cl_2$, TEOA solution (1.5×10^{-3} mol/L), 4 mL acetonitrile, 5 mg catalyst	151.1 (CO)	S1
2D/2D FeNi-LDH/g-C_3N_4	300 W Xe-lamp, 0.084 g $NaHCO_3$, 0.3 mL H_2SO_4 (2 mol/L), 0.05 g gas-prepared sample	1.64 (CH_3OH)	S2
g-C_3N_4@CeO_2 (CeO_2 49.7 wt %)	300 W Xe-lamp, 10 mL H_2O, 50 mg catalyst	4.2 (CO)	S3
Bi_2WO_6/RGO/g-C_3N_4	300 W Xe-lamp (λ >420 nm), 50 mg catalyst	15.96 (CO) 2.51 (CH_4)	S4
g-C_3N_4/NiAl-LDH	300 W Xe-lamp (λ >420 nm), 50 mg catalyst	8.2 (CO)	S5
MnO_2/g-C_3N_4	300 W Xe-lamp, 50 mg catalyst	2.04 (CO)	S6
Bi_3NbO_7/g-C_3N_4	CEL-HXF300, H_2O, Na_2CO_3 (1.3 g), H_2SO_4 (2.0 mL), 50 mg catalyst	37.59 (CH_4)	S7

Table S2. Energy (eV) of groups and Zero Point Energy (ZPE) and TS (T: Temperature, S: Entropy) contributions to the free energies at the standard conditions.

Species	E/eV	ZPE/eV	TS/eV
CO_2	-22.98	0.31	0.66
CO	-14.79	0.13	0.60
H_2O	-14.21	0.56	0.67
H_2	-6.76	0.27	0.40
$*CO_2$	--	0.17	0.24
*COOH	--	0.52	0.11
*CO	--	0.31	0.14

Table S3. Energies (eV) of the Bulk CN surface and corresponding groups.

Bulk CN	Slab (*)	$*CO_2$	*COOH	*CO	CO
E/eV	-950.42	-973.63	-975.76	-965.44	/
ΔE/eV	0.00	-0.23	1.25	-0.51	0.23
ΔG/eV	0.00	0.05	1.79	-0.79	-0.41
G/eV	0.00	0.05	1.84	1.05	0.64

Table S4. Energies (eV) of the CSCN surface and corresponding groups.

CSCN	Slab (*)	*CO_2	*COOH	*CO	CO
E/eV	-942.68	-966.43	-970.17	-957.62	/
ΔE/eV	0.00	-0.77	-0.36	1.72	0.15
ΔG/eV	0.00	-0.49	0.18	1.43	-0.49
G/eV	0.00	-0.49	-0.30	1.13	0.64

References

[S1]***Chin. J. Catal.***, 2022, 43, 1306-1315.

[S2]***Acta Phys. -Chim. Sin.***, 2021, 37, 2010073.

[S3]***Appl. Catal. B***, 2019, 243, 566-575.

[S4]***Appl. Catal. B***, 2018, 239, 586-598.

[S5]***ACS Appl. Mater. Interfaces***, 2018, 10, 2667-2678.

[S6]***Carbon***, 2017, 120, 23-31.

[S7]***Chin. J. Catal.***, 2022, 43, 246-254